Signatures of localization in the effective metallic regime of high-mobility Si MOSFETs

S. Das Sarma,[1] E. H. Hwang,[1,2] K. Kechedzhi,[1] and L. A. Tracy[3]

[1]*Condensed Matter Theory Center and Joint Quantum Institute, University of Maryland, College Park, Maryland 20742, USA*

[2]*SKKU Advanced Institute of Nanotechnology and Department of Physics, Sungkyunkwan University, Suwon, 440-746, Korea*

[3]*Sandia National Laboratories, Albuquerque, New Mexico 87185, USA*

(Received 16 June 2014; revised manuscript received 8 August 2014; published 8 September 2014)

Combining experimental data, numerical transport calculations, and theoretical analysis, we study the temperature-dependent resistivity of high-mobility two-dimensional (2D) Si MOSFETs to search for signatures of weak localization induced quantum corrections in the effective metallic regime above the critical density of the so-called two-dimensional metal-insulator transition (2D MIT). The goal is to look for the effect of logarithmic insulating localization correction to the metallic temperature dependence in the 2D conductivity so as to distinguish between the 2D MIT being a true quantum phase transition versus being a finite-temperature crossover. We use the Boltzmann theory of resistivity including the temperature-dependent screening effect on charged impurities in the system to fit the data. We analyze weak perpendicular field magnetoresistance data taken in the vicinity of the transition and show that they are consistent with weak localization behavior in the strongly disordered regime $k_F\ell \gtrsim 1$. Therefore, we supplement the Boltzmann transport theory with a logarithmic in temperature quantum weak localization correction and analyze the competition of the insulating temperature dependence of this correction with the metallic temperature dependence of the Boltzmann conductivity. Using this minimal theoretical model, we find that the logarithmic insulating correction is masked by the metallic temperature dependence of the Boltzmann resistivity and therefore the insulating $\ln T$ behavior may be apparent only at very low temperatures which are often beyond the range of temperatures accessible experimentally. Analyzing the low-T experimental Si MOSFET transport data, we identify signatures of the putative insulating behavior at low temperature and density in the effective metallic phase.

DOI: 10.1103/PhysRevB.90.125410 PACS number(s): 71.30.+h, 72.15.Rn, 73.63.−b

I. INTRODUCTION

Si metal-oxide-semiconductor field effect transistors (Si MOSFETs) support a highly conductive two-dimensional electron gas (2DEG) system where coupling to a metallic gate allows tuning of electron density in the 2DEG over a wide range. Decreasing density can drive the 2DEG from a highly conductive "metallic" state to a highly resistive "insulating" state [1]. Intense theoretical and experimental research over several decades suggested a number of possible physical mechanisms underlying such behavior in 2DEGs depending on microscopic details of the structure. The subject of the 2D metal-to-insulator transition (2D MIT) arising from the gate-induced tuning of the 2D carrier density is still an active area of research [2], particularly in the context of high-quality (i.e., high-mobility) 2D systems where the transition occurs at relatively low critical density where electron-electron interaction effects may play an important role. In particular, the specific question of whether the density-tuned 2D MIT is or is not a zero-temperature quantum phase transition, as opposed to a crossover from a high-density apparent metallic phase to a low-density insulating phase, has been much debated in the recent literature [2]. If the 2D MIT turns out to be a true quantum phase transition rather than a finite-temperature crossover, one immediate important implication would be that the high-density 2D metallic phase must necessarily be a non-Fermi liquid because a noninteracting 2D disordered Fermi liquid is an insulator at $T = 0$ [2,3].

Early measurements of 2D resistivity in low density Si MOSFETs showed good agreement with the scaling theory of Anderson localization originating from quantum interference of electrons scattered by random disorder potential (see Refs. [1,2], and references therein). The theoretical argument [3] relies on the scaling theory of localization that shows that the system-size-independent semiclassical Boltzmann (or Drude) resistivity ρ_B in two dimensions is overpowered by the logarithmic quantum correction $\sim\frac{1}{\pi}\ln\frac{L}{\ell}$ (in units of h/e^2) arising from quantum interference of diffusing electrons, here L is the system size and ℓ is the electron mean free path. As a result, in the thermodynamic limit all states are localized [3] in a 2D orthogonal class system (preserving time-reversal and spin-rotation symmetries). This result, that all disordered 2D systems are insulating at $T = 0$ in the infinite-system-size limit, was initially derived for noninteracting electrons, but is universally thought to be valid in the presence of weak electron-electron interaction. Boltzmann resistivity can be varied by tuning the electron density in the 2DEG resulting in a tunable apparent metal-insulator transition which occurs when the system size $L = \xi$ equals a characteristic localization length at which the quantum correction equals the Boltzmann part of the resistivity $\rho_B \sim h/e^2$. This is of course a finite-system-size induced crossover (and not really a transition) from an effective apparent 2D metallic phase for $L \ll \xi$ to an insulator for $L \gg \xi$. Experimentally, however, the system-size induced transition is impractical to implement, and one uses carrier density to tune the effective localization length. This is possible because the effective localization length $\xi \sim \ell\exp(\pi k_F\ell/2)$ depends on the underlying 2D carrier density through k_F and through the density-dependent mean-free path ℓ, and thus the 2D MIT can be tuned by changing the carrier density leading to a critical density defining the crossover between the effective metal and the strongly localized insulator.

In realistic experiments, there are inevitably inelastic scattering processes that limit the coherent diffusion of electrons and introduce a temperature-dependent dephasing length $L_\varphi \sim T^{-p/2}$. This dephasing length limits the effective system size in the scaling theory of localization providing a temperature-dependent length scale cutoff (i.e., the system size gets replaced by the dephasing length in the scaling theory) which results in a logarithmic temperature dependence of the quantum correction to resistivity. Therefore, in a resistivity measurement, the metal-insulator transition is evidenced by the qualitative change in the temperature dependence of resistivity with changing electron density from a metallic (or, strictly speaking, weak localization) dependence $\rho^{-1}(T) \approx \rho_B^{-1} - \text{const} \times \ln T$ to an exponential insulating dependence $\rho(T) \sim \exp[(\frac{T_0}{T})^\alpha]$, characteristic of hopping or activated conduction, with some nonuniversal scale T_0 and $\alpha = \frac{1}{3}, \frac{1}{2}, 1$ depending on the details. The presence of weak Coulomb interaction is not expected to change the character of the quantum correction (at least from the point of view of the perturbation theory in the high-density regime) and only affects the coefficient in front of $\ln T$ due to the additional scattering of electrons on Friedel fluctuations of density around impurities [4–10] (the so-called Altshuler-Aronov effect).

By contrast, high-mobility Si MOSFETs $\mu \gtrsim 20\,000$ cm^2/Vs as well as a number of other high-mobility 2DEGs seem to demonstrate a qualitatively different dependence of resistivity $\rho(T,n)$ on electron density n and temperature [2]. In these samples, the low-density conductivity has the standard insulating exponential temperature dependence. However, with increasing density the temperature dependence of resistivity gradually changes from exponential insulating behavior $d\rho/dT < 0$ to a metallic-type $d\rho/dT > 0$ dependence [2,11–19] without any obvious manifestation of the $\ln T$ behavior on the metallic side. Thus, there exists a range of densities where at the lowest accessible temperatures only a metallic temperature dependence is observed $d\rho/dT > 0$. Actually, this metallic temperature dependence (i.e., $d\rho/dT > 0$) typically saturates at low temperatures ($T \lesssim 100$ mK) with the resistivity generically becoming temperature independent (i.e., $d\rho/dT = 0$) at low enough temperatures for all 2D effectively metallic samples. Whether this low-temperature resistivity saturation (with the actual value of the saturated low-temperature residual resistivity being dependent on the carrier density) is a fundamental phenomenon arising from some incipient low-energy cutoff suppressing the effective metallicity or is just a trivial manifestation of electron heating effect (where the carrier temperature saturates and no longer decreases with the decreasing lattice temperature) is not known definitively.

In addition to this low-temperature resistivity saturation, there is a higher-temperature anomaly in the metallic behavior also; typically, the 2D metallic resistivity $\rho(T)$ starts decreasing (i.e., $d\rho/dT < 0$) at some density-dependent "high" temperature (1–10 K) after manifesting the metallic (i.e., $d\rho/dT > 0$) behavior and before phonon scattering effects take over at still higher temperatures. The combination of metallic (i.e., $d\rho/dT > 0$) behavior at low temperatures and insulating (i.e., $d\rho/dT < 0$) behavior at intermediate temperatures coupled with phonon-induced metallic behavior (i.e., $d\rho/dT > 0$) at still higher temperatures could lead to a rather interesting nonmonotonicity in $\rho(T)$ on the metallic side of the 2D MIT at low carrier densities, and has been well studied in the literature [20]. The higher-temperature effective insulating behavior in the metallic phase is thought to arise from a quantum-classical crossover phenomenon in the 2D system occurring on the scale of the Fermi temperature ($\propto n$) which could be low ($\lesssim$10 K) at the low carrier densities of interest for the 2D MIT phenomena [21]. We will not much discuss this temperature-induced quantum-classical high-temperature transition from metallic to insulating behavior in this paper, concentrating instead on the density-induced 2D MIT transition at low temperatures. The sign of the derivative switches from insulating to metallic at a value of resistivity of the order of the resistance quantum $\rho \sim h/e^2$, i.e., at the value at which a transition to strong localization behavior is predicted by the scaling theory. On the metallic side of this transition, where $d\rho/dT > 0$, the resistivity increases sharply by a factor of $\gtrsim$2–3 with growing temperature at lower carrier density staying within the metallic phase. This pronounced temperature dependence diminishes with growing density deeper in the metallic regime. Standard $\ln T$ quantum corrections are observed at high densities where the metallic temperature dependence is weak [10,22,23]. By contrast, in the vicinity of the metal-insulator transition, logarithmic corrections are typically not observed within the experimentally accessible temperature range. This qualitative change in the temperature dependence of 2D resistivity driven by electron density is routinely called a metal-insulator transition in the literature and we will use this convention in the following despite the ongoing debate about the existence or not of an actual thermodynamic phase transition at this point [2]. Our view in the current work is based on the assumption that the 2D MIT is a crossover phenomenon with the $\ln T$ behavior suppressed by the strong metallic temperature dependence of the Drude-Boltzmann resistivity at lower metallic densities. We will critically test this assumption in this paper by comparing theory and experiment in the density- and temperature-dependent transport data in high-mobility Si MOSFETs.

An important distinction between low- and high-mobility samples is in the relative strength of Coulomb interactions. The presence of weaker disorder in high-mobility structures allows for metallic behavior to persist down to very low densities $n \sim 10^{11}$ cm^{-2} which correspond to very small values of Fermi energy and thus large values of the density-dependent dimensionless interaction strength in the system which may be as large as $r_s \equiv 1/\sqrt{\pi n a_B^2} \sim 10$. Here, $a_B = \hbar\kappa/(me^2)$ is the effective Bohr radius of electrons in the 2DEG, κ being the background dielectric constant. We note, however, that even high-density Si MOSFETs, which were extensively studied [1] before the current interest arose in the 2D MIT phenomena, have a dimensionless interaction strength $r_s > 1$, and 3D metals all have $r_s \sim$ 4–7. Thus, it is not manifestly clear that interaction by itself is the sole physical mechanism underlying the 2D MIT phenomena. Perhaps an even more important aspect of high-mobility 2D samples in the context of strong metallic temperature dependence of resistivity is that, by having a relatively low critical density distinguishing the metallic and the strongly insulating regimes

by virtue of low-sample disorder (and hence high-sample mobility), the Fermi temperature ($T_F \propto n$) is low ($\sim$1–10 K) in high-mobility samples in the metallic regime. Then, the low-temperature regime ($T \approx 0.1$–5 K) where the 2D metallic behavior manifests itself (i.e., large positive $d\rho/dT$) has effectively large values of the dimensionless temperature $T/T_F \sim 1$. By contrast, 3D metals, which are also strongly interacting electron systems by virtue of having $r_s \gg 1$ have very low dimensionless effective temperature $T/T_F \sim 10^{-4}$, by virtue of $T_F \sim 10^4$ K in metals. The large effective values of T/T_F also distinguish the high-mobility 2D systems from the low-mobility 2D systems where the Fermi temperature is $T_F \gtrsim 100$ K in the metallic phase and thus $T/T_F \sim 10^{-2}$–10^{-3} in the low-temperature experimental regime.

Extensive theoretical work demonstrated that all of the observed features of the temperature dependence of resistivity on the metallic side of the metal-insulator transition can be successfully described extrapolating from high densities (and coincidentally low interactions strength) and using a Boltzmann transport theory which includes the temperature-dependent screening [21,24,25] of charged impurities. The metallic increase of the resistivity with growing temperature is explained by a decreasing efficiency of screening by the electron gas of charged impurities with growing temperature. The large effective value of T/T_F explains the experimentally observed large $d\rho/dT$ in the metallic phase. This suggests that the standard Fermi-liquid theory may explain the unusual temperature and density dependence of resistivity in high-mobility Si MOSFETs. However, the Fermi-liquid theory also predicts the presence of quantum corrections giving rise to $\ln T$ behavior which are not observed experimentally in the vicinity of the metal-to-insulator transition. The observation and analysis of these $\ln T$ corrections would allow us to continuously connect the low-density strong interaction and strong disorder regime to the weakly interacting high-density Fermi-liquid regime where the Boltzmann theory is valid. There may be a simple conventional explanation for the absence of quantum corrections in the data. Analyses of the high-density data [22,23,26,27] where $\ln T$ is observed suggest that at low densities in high-mobility samples the temperature at which $\ln T$ would become apparent may be beyond the measurement temperatures because of electron heating [27,28]. Our approach in this paper is a straightforward phenomenological approach where we assume that the metallic transport has contributions from both the screening-induced semiclassical metallic temperature dependence and the weak localization induced quantum $\ln T$ temperature dependence. The strong metallic temperature dependence of the resistivity completely overwhelms the $\ln T$ insulating correction at higher temperatures with the logarithmic correction eventually manifesting itself at some density-dependent low temperatures which might very well be inaccessible to experimental measurements due to electron heating problem. We also present experimental transport data on 2D MIT in Si MOSFET samples which are consistent with the presence of both screening-induced metallic temperature dependence and quantum weak localization correction.

In this paper, we present experimental resistivity data taken on two high-mobility Si MOSFETs demonstrating 2D metal-insulator transition. We construct a microscopic Boltzmann theory of resistivity in Si MOSFETs that includes the effect of temperature-dependent screening of charged impurities by the electron gas. We use this model to fit the metallic temperature dependence observed in the data. We then construct a minimal additive model describing the competition between this metallic temperature dependence of resistivity and the insulating temperature dependence due to the quantum correction. Using this model, we determine the temperatures at which the quantum correction to resistivity is expected to dominate the experimental data which turn out to be beyond the range of the current experiments. We also discuss the magnetoresistance data on the two samples in the vicinity of the transition and show that they are qualitatively consistent with weakly interacting localization theory suggesting that the standard Fermi-liquid theory could be sufficient to describe the temperature dependence of the transport properties in high-mobility Si MOSFETs.

II. DESCRIPTION OF THE EXPERIMENT

We consider the transport data on two Si MOSFET samples with relatively high mobility: sample A ($\mu = 1.5 \times 10^4$ cm^2/Vs) and sample B ($\mu = 10^4$ cm^2/Vs). The resistivity temperature dependence at various carrier densities is shown in Fig. 1. At the lowest densities, an insulating exponential temperature dependence is observed. This insulating behavior $d\rho/dT < 0$ gradually loses exponential character with increasing density. At higher densities, the temperature dependence of resistivity becomes nonmonotonic: with increasing temperature, the resistivity drops down to a minimum value and then rises up $d\rho/dT > 0$ to a maximum before gradually sloping downwards. There is a range of densities at which at the

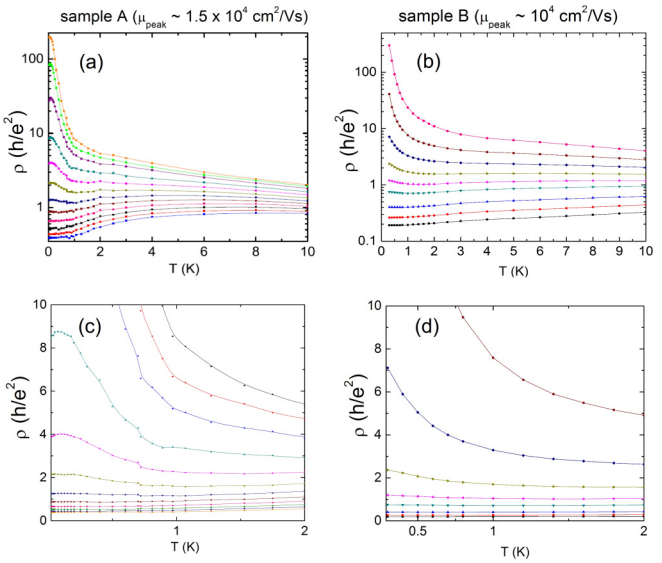

FIG. 1. (Color online) Resistivity as a function of temperature for sample A and B plots [(a) and (c)] and [(b) and (d)], respectively, showing zoom-in of the low-temperature region in (c) and (d). Different lines correspond to different carrier density n in units of 10^{11} cm^{-2} (from top to bottom): in (a) and (c) $n =$ 1.07, 1.10, 1.13, 1.20, 1.26, 1.32, 1.38, 1.44, 1.50, 1.56, 1.62, and 1.68; in (b) and (d) $n =$ 1.52, 1.70, 1.88, 2.05, 2.23, 2.41, 2.76, 3.11, and 3.46. Plot (a) is reproduced from Ref. [29].

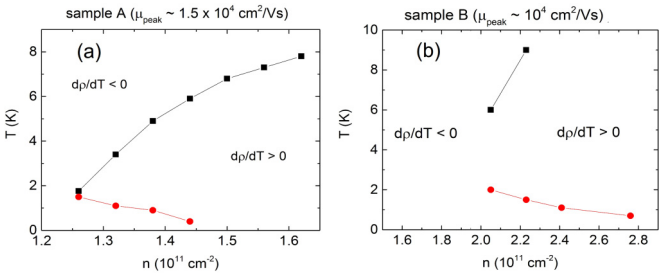

FIG. 2. (Color online) Black squares and red circles correspond to the maximum and minimum of the measured resistivity $\rho(T)$ in Fig. 1, respectively.

lowest accessible temperatures there is no sign of the insulating rise of the resistance or $\ln T$ metallic correction. This form of temperature dependence $\rho(T)$ is typical in high-mobility Si MOSFETs [11–18]. We point out, as is obvious from Figs. 1(c) and 1(d) where the resistivity is shown on an expanded temperature scale, the insulating temperature dependence is suppressed gradually as density increases and there is really no absolutely sharp density distinguishing metallic and insulating behaviors.

In Fig. 2, we track the evolution with electron density of the temperatures at which the maximum and minimum of the resistivity are reached. Red circles here correspond to the low-temperature resistivity minimum which signifies the onset of insulating behavior. The black squares correspond to the high-temperature maximum of the resistivity. Our interest in this work is mostly on the red circles which provide the temperature at which the metallic temperature dependence is just being overcome by the quantum localization effect on the effective metallic side of the 2D MIT. We note that as expected this characteristic temperature for the resistivity minimum is rather low and it increases with decreasing density as localization effects become more important quantitatively. The black squares in Fig. 2, indicating the resistivity maxima in $\rho(T)$ as a function of carrier density, provide the characteristic temperature for the high-temperature quantum-to-classical crossover in the 2D transport as discussed in Sec. I. This quantum-classical crossover typically occurs on the scale of the Fermi temperature (typically around $T \sim T_F/2$) and therefore decreases with decreasing carrier density. The region in-between the red circles and the black squares is the putative 2D effective metallic phase where the metallic temperature dependence with $d\rho/dT > 0$ is manifested in 2D transport. We note that in the high-mobility samples, the regime (below red circles) showing $\ln T$ weak localization behavior is strongly suppressed by the metallic temperature dependence arising from other physical mechanisms.

III. BOLTZMANN THEORY

Strong disorder and strong interaction low-density regime is difficult to address theoretically. Boltzmann theory allows us to quantitatively describe mobility dependence on the electron density in a wide density regime (of not too low densities so that one is away from the strongly localized regime). The model of disorder describing the density dependence of mobility is a combination of random charged impurities and surface roughness [1]. This Boltzmann theory quantitatively agrees with mobility measurements in a wide density range in the high-density metallic regime [29]. It is therefore natural to extrapolate this theory to the low-density regime of strong disorder and interaction. At very low densities, the effect of surface roughness is negligible and the resistivity is completely dominated by charged impurities [1]. In the following, we neglect the effect of surface roughness, but our results do not change if surface roughness is included in the theory since it has little quantitative effect on transport at the low carrier densities of interest in this work.

Boltzmann conductivity σ_B is given by

$$\rho_B^{-1} \equiv \sigma_B = ne^2\langle\tau\rangle/m, \tag{1}$$

where n is the electron density, m is the effective mass of electrons, and the average transport time $\langle\tau\rangle$ reads as

$$\langle\tau\rangle \equiv \frac{\int dE\,\tau(E)E\left(-\frac{\partial f}{\partial E}\right)}{\int dE\,E\left(-\frac{\partial f}{\partial E}\right)}. \tag{2}$$

Here, the impurity-averaged relaxation time $\tau(E)$ is given by

$$\frac{1}{\tau(E_k)} = \frac{2\pi}{\hbar}\sum_{\alpha,\mathbf{k}'}\int_{-\infty}^{\infty} dz\,N_i(z)|u(\mathbf{k}-\mathbf{k}';z)|^2 \times(1-\cos\theta_{\mathbf{k}\mathbf{k}'})\delta(E_k - E_{k'}), \tag{3}$$

where the standard parabolic energy dispersion is assumed for E_k, $N_i(z)$ is the 3D charged impurity density, and $u(\mathbf{q};z)$ is the 2D Fourier transform in the plane of the 2DEG of the impurity potential screened by the electron gas,

$$u(q;z) = \frac{1}{\varepsilon(q)}\frac{2\pi e^2}{\kappa q}F_{\rm imp}(q;z), \tag{4}$$

where κ is the background dielectric constant, and $F_{\rm imp}(q;z)$ is a form factor depending on the microscopic details which are known [1]. In the strictly 2D limit, an impurity charge located a distance d away from the 2DEG is described by a form factor $F_{\rm imp} = e^{-qd}$. The screening effect is characterized by the dielectric function $\varepsilon(q)$ calculated in the random phase approximation (RPA) [1].

The resulting theory fits well (see Fig. 3) the strong non-monotonic temperature dependence of the metallic resistivity

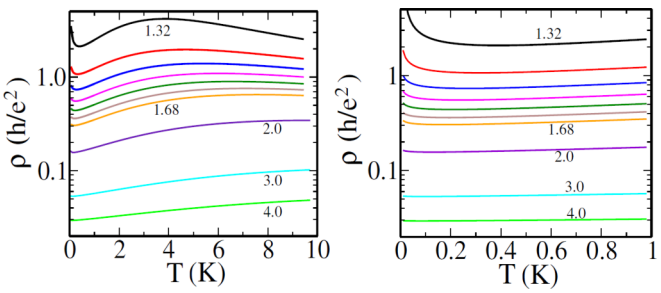

FIG. 3. (Color online) Boltzmann resistivity theory for parameters of sample A (from fitting) combined with the weak localization correction (7). Numbers on the plot correspond to the electron density in units of 10^{11} cm^{-2}. The right panel shows a zoom-in on a low-temperature region in the left panel.

at low densities [21,24]. To reproduce the experimental data, we adjust the density of impurities and their locations in the oxide layer in a narrow range of values as free-fitting parameters and the resulting model reproduces the functional dependence of the resistivity on temperature and electron density in the 2DEG. We mention that the oxide impurity charge density and their spatial distribution necessary to get agreement between the theory and the experimental resistivity data are very reasonable (and independently confirmed by capacitance measurements). The details of this comparison between theory and experiment for our samples are given in Ref. [29] and not repeated here. The nonmonotonicity of the temperature dependence of resistivity as a function of density can therefore be explained within this model: with increasing temperature screening becomes less effective and as a result the resistivity increases. The increase in resistivity can be by a factor 2–3 in this regime due to the temperature-induced weakening of the screening effect which explains the observed metallic temperature dependence. At higher temperatures, the quantum-to-classical crossover results in the decreasing resistivity with temperature at $T/T_F \sim 1$. The theoretical details of the screening model for the 2D resistivity and the corresponding comparisons with experimental "metallic" temperature dependence of transport properties have already been discussed extensively in earlier references [20,21,24,25,29] and will not be repeated here. We mention, however, that none of these earlier references included the weak localization effect into consideration (as we do in this work) assuming the effective metallic behavior to dominate the transport properties completely.

Extrapolation to the strong interaction regime makes sense since the random phase approximation (RPA) is given by a subset of the most divergent diagrams which therefore may dominate even at strong interactions [21,24]. Extrapolation of Boltzmann theory to low density and strong interaction may be successful as it describes short-range phenomena $\lesssim \ell$ (where ℓ is the mean-free path) as opposed to localization physics and localizing interaction correction originating from the diffusive length scales $\gg \ell$. Boltzmann theory therefore may describe the case of strong dephasing and/or high temperature. In particular, the fact that the effective temperature is high (i.e., $T/T_F \sim 1$) in the low-density high-mobility samples makes 2D MIT a high-temperature crossover phenomenon where interaction effects are likely to be strongly suppressed by temperature. We note here (as can be seen in Fig. 1) that at very low temperatures, the temperature dependence of the metallic resistivity invariably saturates, thus making the 2D MIT an effectively high-temperature phenomenon.

IV. MAGNETORESISTANCE

A strong indication of a Fermi-liquid behavior in the strong disorder and strong interaction regime near the metal-insulator transition is the observation of weak perpendicular field magnetoresistance which is a smoking gun signature of the weak localization physics. Magnetoresistance data taken on sample A (see Fig. 5 in Ref. [29]) were fitted using the standard digamma function expression for the weak localization theory

$$\frac{\delta\rho}{\rho^2} = -\alpha g_v G_0 \left[\Psi\left(\frac{1}{2}+\frac{\tau_B}{\tau}\right) - \Psi\left(\frac{1}{2}+\frac{\tau_B}{\tau_\varphi}\right)\right], \qquad (5)$$

where $\tau_B \equiv \hbar/(4eBD)$, $G_0 = \frac{e^2}{2\pi^2\hbar}$, B stands for the perpendicular magnetic field, D the diffusion coefficient, g_v the valley degeneracy factor. The coefficient α along with the dephasing time τ_φ are used as fitting parameters with the best fit achieved with $\alpha \approx 0.25$ and $\tau_\varphi = 33, 32$, and 28 ps for electron densities $n = 1.45, 1.51$, and 1.63×10^{11} cm^{-2} at $T = 0.1$ K ($g_v = 1$ is assumed in the fits).

In this low-density regime of these measurements the resistivity is high $\rho \lesssim h/e^2$, which suggests $k_F\ell \gtrsim 1$, whereas the standard weak localization theory is really valid for $k_F\ell \gtrsim 10$. Therefore, extra care has to be taken when interpreting these results and quantum corrections of higher order in $1/(k_F\ell)$ may have to be considered going beyond the usual weak localization theory. The key effect of the higher-order terms is in lowering the prefactor in front of the magnetoresistance expression (5) from $\alpha = 1$ to $\alpha \approx 1 - \beta(G_0\rho)$, with β a degeneracy factor depending on the intervalley scattering in the system. This reduction in α is a result of the two-loop correction to noninteracting weak localization theory [30]. Also, an additional magnetoresistance due to electron-electron interactions may enhance the reduction of the prefactor with the combined effect leading to $\alpha \approx 1 - 2\beta(G_0\rho)$, as discussed in Ref. [30].

Intervalley scattering due to the short-range scattering may suppress the valley degeneracy factor g_v in front of the magnetoresistance in Eq. (5). The effect of intervalley scattering on magnetoresistance was analyzed in great detail using high-density measurements in high-mobility Si MOSFETs in Ref. [31]. The typical intervalley scattering times extracted from these measurements are in the range 1 ps $\lesssim \tau_v \lesssim$ 20 ps. Comparing the typical values of τ_v with the dephasing time $\tau_\varphi \sim 30$ ps in our samples extracted from our measurements we conclude that $\tau_v/\tau_\varphi \lesssim 1$ and valley mixing is relatively strong and the effective degeneracy factor is expected to be in the range $1 \lesssim g_v$ in Eq. (5). This means that the fitting parameter $\alpha g_v = 0.5$ in Eq. (5) signifies a reduction of the magnetoresistance amplitude by at least a factor of 2, and probably more. This suggests that the data in our Si MOSFETs are qualitatively consistent with the detailed theory [30] of quantum corrections in a weakly interacting strongly disordered Fermi liquid in the presence of strong intervalley scattering (which may arise from the surface roughness at the Si-SiO_2 interface providing short-range scattering). This agreement has to be taken with a grain of salt as the interaction strength in the low-density regime may not be small. Nevertheless, similar magnetoresistance behavior was observed in other high-mobility Si MOSFET measurements [32] and other 2DEGs [33–35] giving us confidence in this conclusion.

Experimental values of the magnetoresistance cutoff extracted from the fitting procedure give a dephasing time $\tau_\varphi(0.1\text{ K}) \sim 30$ ps in our sample, which is an order of magnitude shorter than the value expected due to inelastic electron-electron scattering in the diffusive regime [4,5,36]

$$\frac{\tau}{\tau_\varphi} = \gamma \frac{k_B T}{E_F} \ln g, \qquad (6)$$

where γ is a factor of the order unity. Despite the low-mobility 2D devices showing quantitative agreement with the dephasing rate due to inelastic electron-electron interaction [37,38] in Eq. (6), and also high-density high-mobility devices showing quantitative agreement with the dephasing rate formula [31], low-density measurements routinely manifest an order of magnitude shorter dephasing times than predicted by Eq. (6) [32], which cannot be explained by simple deviations [30] from Eq. (6) at strong disorder $k_F\ell \sim 1$. The same enhanced dephasing rate is also routinely observed in other 2DEGs [33–35]. It seems likely that either there is an additional dephasing mechanism responsible for such short dephasing rates or the magnetoresistance is cut off by the localization length. At low values of $k_F\ell \gtrsim 1$, the localization length $\xi \approx \ell \exp(\pi k_F \ell/2)$ becomes comparable to the dephasing length. It has been shown theoretically that Eq. (5) is applicable even for $\xi < L_\varphi$ as long as $k_F\ell > 1$. However, the meaning of the dephasing rate extracted from the data is different in this regime since the localization length cuts off the magnetoresistivity instead of dephasing [30]. This may cause a saturation in the temperature dependence of the dephasing rate. It is, in principle, also possible that the dephasing rate at very low carrier density is dominated by the physics of density inhomogeneity [39] (i.e., disorder-induced puddles) not included in the theory leading to Eq. (6).

V. TEMPERATURE DEPENDENCE OF RESISTIVITY WITHIN THE FERMI-LIQUID MODEL

High-density measurements identified standard $\ln T$ quantum correction to 2D resistivity [22,23,32]. It is therefore natural to expect that, since the Boltzmann theory can be continuously extended to low densities, the $\ln T$ correction is present in the system at all densities in addition to the Boltzmann contribution. The presence of weak field magnetoresistance discussed above is an additional argument in favor of the Fermi-liquid behavior at low densities near the metal-insulator transition. Therefore, we assume the presence of $\ln T$ quantum correction to the Boltzmann resistivity up to the onset of the strongly insulating behavior [22,26,27]. However, with decreasing electron density, the metallic temperature dependence of the Boltzmann resistivity becomes pronounced. As a result, there is a competition between the insulating and metallic temperature dependence at low densities which are simultaneously present since they arise from distinct microscopic mechanisms. We consider the minimal model of transport that describes this behavior, including both semiclassical Boltzmann contribution and the quantum weak localization contribution

$$\rho(T) = \frac{1}{\rho_B^{-1}(T) + \sigma_{WL}(T)}, \tag{7}$$

where $\rho_B(T)$ is the temperature-dependent Boltzmann resistivity given by Eq. (1). The quantum correction to conductivity in Eq. (7) is given by the standard theory

$$\sigma_{WL} = -g_v G_0 \frac{1}{2\pi} \ln \frac{\tau_\varphi}{\tau}. \tag{8}$$

Figure 3 shows the calculated temperature and density dependence of the resistivity for the parameters extracted from the fits of the data for sample A. In Fig. 4, we present the theoretical results corresponding to those shown in Fig. 2. It is clear that the theoretical results in Fig. 4 closely resemble the experimental results shown in Fig. 2 for sample A, thus demonstrating that 2D MIT may indeed be a crossover phenomenon. Here, the logarithmic correction becomes apparent only below the experimentally accessible temperatures $T \sim 0.1$ K, which is qualitatively similar to the experimental situation.

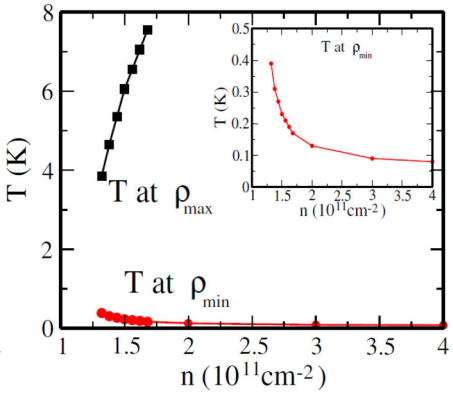

FIG. 4. (Color online) Black squares and red circles correspond to maximum and minimum of $\rho(T)$ in Eq. (7). Inset shows temperature at the minimal value of resistance as a function of electron density.

In Fig. 5, we present the theoretical calculation for the parameters corresponding to the experimental sample B, which qualitatively simulates the experimental results for sample B shown in Figs. 1(b), 1(d), and 2(b). Comparison of Figs. 1 and 2

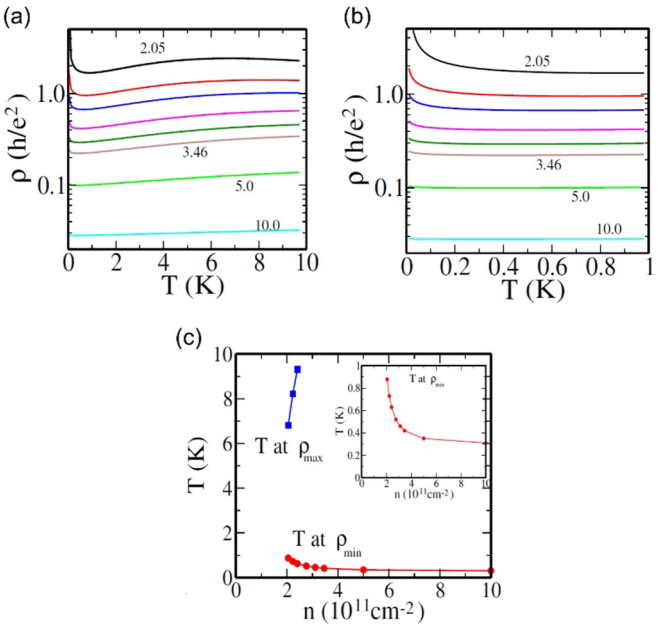

FIG. 5. (Color online) Theoretical results for resistivity as a function of temperature for parameters of sample B showing a zoom-in of the low-temperature region in (b) of the results in panel (a). (c) Red circles and black squares correspond to numerical calculation of the minimum and maximum in the temperature dependence of resistivity for sample B, respectively.

with Figs. 3–5 establishes that the crossover picture of 2D MIT is valid qualitatively (and probably even quantitatively), i.e., both the screening-induced metallic temperature dependence and the quantum weak localization temperature dependence are present in the resistivity.

VI. DISCUSSION AND CONCLUSION

In this paper, we present experimental and theoretical results for the density-dependent low-temperature transport properties of high-mobility 2D Si MOSFETs manifesting the 2D MIT phenomena with the critical goal of searching for the possible presence of the quantum weak localization (i.e., $\ln T$) corrections to the resistivity on the apparent metallic side of the so-called 2D metal-insulator transition. Our detailed analyses of the experimental transport data indicate the existence of a resistivity minimum at a density-dependent characteristic low temperature in the effective metallic regime. The existence of this characteristic temperature, with resistivity $\rho(T)$ increasing with both increasing and decreasing temperature away from this minimum, points to the presence of two competing transport mechanisms in the system with one being "metallic" (i.e., $d\rho/dT > 0$) and the other "insulating" (i.e., $d\rho/dT < 0$) which balance each other at this low-T resistivity minimum with the localization effect dominating at still lower temperatures. We identify the two competing mechanisms to be the temperature-induced reduction of screening (leading to the metallic $d\rho/dT > 0$ behavior) and the quantum interference induced weak localization contribution (leading to the $\ln T$ weak localization correction with $d\rho/dT < 0$) which dominate, respectively, the higher and the lower temperature sides of the resistivity minima. We find that the minimum occurs mostly at temperatures which are experimentally inaccessible in high-mobility samples (due to perhaps the well-known electron heating problem in 2DEG semiconductors), thus providing a possible explanation for why most experimental measurements in high-mobility samples do not manifestly show the $\ln T$ insulating behavior at low temperatures in the metallic regime. We believe that the $\ln T$ weak localization behavior would routinely show up in the metallic transport properties of high-mobility samples if much lower experimental electron temperatures can be achieved in future measurements. In fact, our work indicates that the most straightforward experimental technique to search for signatures of localization in the metallic regime of high-mobility 2D semiconductor systems is to look for extrema in the resistivity $\rho(T)$ at a fixed density n by numerically obtaining the solutions of $d\rho/dT = 0$ in the experimental $\rho(T,n)$ data at fixed density. The low-temperature minima in the resistivity would correspond to the temperature at each density below which localization correction dominates the semiclassical metallic temperature dependence. Depending on the carrier density, this minimum could lie at inaccessibly low temperature, but there still should be some signatures for the minima in the data. As observation of this low-temperature density-dependent minima (Fig. 2 in our samples) in the transport data indicates that the 2D MIT is a crossover and not a true quantum phase transition, and the absence of a manifest $\ln T$ weak localization effect in the resistivity is simply a feature of the insulating localization correction being overwhelmed by a strong metallic temperature dependence in the semiclassical Drude-Boltzmann resistivity as our theoretical results in Figs. 3–5 clearly demonstrate. The excellent qualitative agreement between our theory and our experiment is a strong evidence in favor of 2D MIT being a crossover phenomenon. The possibility of 2D MIT being a Fermi-liquid crossover phenomenon driven by disorder in high-mobility low-density MOSFETs with weak localization effects masked by finite-temperature Drude-Boltzmann effects was also pointed out in the early experimental works of Pudalov [26,28,40] and of Pepper [41,42].

One feature, prominent both in our experimental data Figs. 1 and 2 and in our theory (Figs. 3–5) needs to be specifically mentioned in addition to the resistivity minima discussed before. It is the existence of the high-temperature resistivity maxima in the data (black squares in the figures) with $d\rho/dT < 0$ above this temperature (until phonons become important at still higher temperatures). This quantum-classical high-temperature crossover behavior is ubiquitous in all high-mobility 2D systems in the metallic phase, where after the sharp initial rise of $\rho(T)$ with increasing T, $\rho(T)$ goes through a maximum at a density-dependent "high" temperature slowly decreasing beyond this characteristic temperature until phonon scattering takes over at still higher temperatures. We note that the characteristic temperature for this resistivity maxima (black squares) rapidly decreases with decreasing density, whereas the characteristic temperature for the resistivity minima (red circles) increases with decreasing density. Once these two lines come close together ($n \sim 1.2 \times 10^{11}$ cm^{-2} for sample A and $n \sim 1.8 \times 10^{11}$ cm^{-2} for sample B, see Fig. 2), the system simply behaves as an insulating system at all lower densities since $d\rho/dT < 0$ for all density and temperature below this intersection regime of the black squares and red circles. This finite-temperature behavior is also apparent in our theoretical curves [see Fig. 4 for sample A and Fig. 5(c) for sample B].

Before concluding, we point out that, within our model of Boltzmann resistivity due to screened charged impurity scattering and weak localization due to quantum interference [i.e., Eq. (7) in Sec. V], we can actually derive a leading-order analytical formula for the characteristic temperature (i.e., the red circle plots in the figures) for the resistivity minima below which weak localization effect should dominate the metallic transport properties. Using the leading-order (linear) analytical low-temperature expansion in temperature for $\rho_B(T)$ in Eq. (7) we get for the characteristic temperature T_m where $d\rho/dT = 0$ to be

$$T_m \propto T_F/\sigma_B(T=0), \tag{9}$$

where $T_F \propto n$ is the Fermi temperature and $\sigma_B(T=0) = \rho^{-1}(T=0)$ is the zero-temperature Boltzmann conductivity due to charged impurity scattering. It is well known [43] that $\sigma_B(T=0)$ obeys an approximate scaling law with the carrier density going as

$$\sigma_B \sim n^{\alpha+1}, \tag{10}$$

where $\alpha(n) \approx 0.3$ in Si MOSFETs in the low-density metallic regime. This leads to a rather weak density dependence of the

characteristic temperature T_m going as

$$T_m \sim n^{-0.3}, \tag{11}$$

which is approximately consistent with the experimental and theoretical numerical results for the red circle lines in Figs. 2, 4, and 5(c). The important point to note is that the weak localization correction becomes important at lower density since the weak localization effect becomes progressively stronger with the decreasing Drude conductivity with decreasing carrier density. On the other hand, if $\sigma_B(T)$ is temperature independent as it is for low-mobility samples, the weak localization $\ln T$ correction would be visible at all carrier densities.

We conclude by emphasizing that our theory has many approximations which need to be improved in future work. We neglect effects of interaction in the theory beyond the finite-temperature screening effect by the electrons themselves which we include within RPA (i.e., infinite sum of bubble diagrams). At the low carrier densities of interest in the 2D MIT problem, interaction effects are likely to be important, but we neglect them in the spirit of obtaining the leading-order result within the minimal model. In addition, we believe that the interaction effects may be substantially suppressed by finite temperature since T/T_F is not particularly small at the experimental densities and temperatures. We also assume rather unrealistically that the weak localization quantum correction may simply be added to the Drude-Boltzmann conductivity as a $\ln T$ correction, which is obviously a simplification done in the spirit of developing the minimal physical model for including both metallic and insulating temperature dependence within a single unifying scheme. In particular, neither the Boltzmann theory nor the simple weak localization correction is strictly applicable in the strongly disordered situation close to the metal-insulator transition where $k_F\ell \sim 1$, but we have assumed in this work that such a minimal theory (i.e., Boltzmann conductivity along with the $\ln T$ weak localization quantum correction) can be continuously extended from the high-density ($k_F\ell \gg 1$) regime to the low-density regime ($k_F\ell \gtrsim 1$) as long as the system is still nominally in the metallic phase. Our minimal theory obviously becomes progressively quantitatively worse as the carrier density decreases, but we think that it remains qualitatively valid all the way down to $k_F\ell \gtrsim 1$ in the metallic phase. We have neglected all phonon scattering effects in the theory which probably become important for $T \gtrsim 10$ K outside the regime of our interest. It is straightforward to include phonon scattering in the theory and it adds a resistivity increasing linearly with T for $T > T_{\rm BG}$ ($\sim$10 K in Si MOSFET) where $T_{\rm BG}$ is the Bloch-Gruneisen temperature. Since our interest in this paper is the low-temperature 2D MIT physics, phonon scattering effects are irrelevant for our problem. A 2DEG in the presence of disorder and electron-electron interaction is expected to manifest a diffusive (Altshuler-Aronov) interaction correction to conductivity [4–10] which gives another (i.e., in addition to the weak localization correction) $\ln T$ contribution in the temperature dependence of conductivity. However, the prefactor in front of $\ln T$ given by a combination of singlet and triplet components is not known at low electron densities of interest in this work since interaction effects are nonperturbatively strong at low carrier densities. This Altshuler-Aronov effect does not change the functional form of the temperature dependence of resistivity, and therefore our theory as described by Eqs. (7) and (8) not including the Altshuler-Aronov part of the electron-electron interaction correction (note that the ballistic part of the electron-electron interaction effect is included in our Boltzmann theory of Sec. III) nevertheless qualitatively describes the data. It is, however, important to point out that naively adding an Altshuler-Aronov $\ln T$ term in our theory will be an incorrect double counting of many-body effects since the screening effect we included nonperturbatively in the theory already contains the Hartree part of the interaction effect in the ballistic regime (which crosses over to the $\ln T$ effect in the diffusive regime [6,7], and thus there is no need to add a separate $\ln T$ term arising from the Altshuler-Aronov effect also.

Finally, we mention that we have not discussed at all the nature of the actual crossover to the strongly localized exponential temperature dependence (in the resistivity) at very low carrier density as our focus in this work has entirely been on the signature of weak localization in the putative metallic regime. The issue of the strong localization crossover has recently been discussed in great detail by the two of us [44]. One key issue that remains open in this context is the role of impurity-induced density inhomogeneity or puddle formation in the 2DEG as the system crosses over to the strongly insulating phase and screening fails completely. Such inhomogeneous puddles could lead to percolation physics competing with the physics of Anderson localization. In fact, sometimes the crossover to the strong localization behavior may itself be considered a percolation transition as was done in Ref. [29]. The interplay of puddle physics and localization physics in the strongly interacting 2D system is an interesting open question in the 2D MIT problem. For our specific considerations, the puddle size could act as a cutoff for the dephasing length explaining why the low-temperature dephasing length appears to be short compared with the standard Fermi-liquid theory.

ACKNOWLEDGMENT

This work is supported by NSA-LPS-CMTC.

[1] T. Ando, A. B. Fowler, and F. Stern, Rev. Mod. Phys. **54**, 437 (1982).

[2] E. Abrahams and M. P. Sarachik, Rev. Mod. Phys. **73**, 251 (2001); B. Spivak, S. V. Kravchenko, S. A. Kivelson, and X. P. A. Gao, *ibid.* **82**, 1743 (2010); S. D. Sarma and E. Hwang, Solid State Commun. **135**, 579 (2005); S. V. Kravchenko and M. P. Sarachik, Rep. Prog. Phys. **67**, 1 (2004).

[3] E. Abrahams, P. W. Anderson, D. C. Licciardello, and T. V. Ramakrishnan, Phys. Rev. Lett. **42**, 673 (1979).

[4] B. Altshuler and A. Aronov, *Electron-Electron Interactions in Disordered Systems* (Elsevier, Amsterdam, 1985).

[5] E. Akkermans and G. Montambaux, *Mesoscopic Physics of Electrons and Photons* (Cambridge University Press, New York, 2007).
[6] G. Zala, B. N. Narozhny, and I. L. Aleiner, Phys. Rev. B **64**, 214204 (2001).
[7] G. Zala, B. N. Narozhny, and I. L. Aleiner, Phys. Rev. B **65**, 020201(R) (2001).
[8] I. V. Gornyi and A. D. Mirlin, Phys. Rev. B **69**, 045313 (2004).
[9] M. S. Burdis and C. C. Dean, Phys. Rev. B **38**, 3269 (1988).
[10] N. N. Klimov, D. A. Knyazev, O. E. Omel'yanovskii, V. M. Pudalov, H. Kojima, and M. E. Gershenson, Phys. Rev. B **78**, 195308 (2008).
[11] T. N. Zavaritskaya and E. I. Zavaritskaya, Pis'ma Zh. Eksp. Theor. Fiz. **45**, 476 (1987) [JETP Lett. **45**, 609 (1987)].
[12] S. A. Vitkalov, H. Zheng, K. M. Mertes, M. P. Sarachik, and T. M. Klapwijk, Phys. Rev. Lett. **87**, 086401 (2001).
[13] Y. Tsui, S. A. Vitkalov, M. P. Sarachik, and T. M. Klapwijk, Phys. Rev. B **71**, 113308 (2005).
[14] S. V. Kravchenko, G. V. Kravchenko, J. E. Furneaux, V. M. Pudalov, and M. D'Iorio, Phys. Rev. B **50**, 8039 (1994).
[15] S. V. Kravchenko, W. E. Mason, G. E. Bowker, J. E. Furneaux, V. M. Pudalov, and M. D'Iorio, Phys. Rev. B **51**, 7038 (1995).
[16] S. V. Kravchenko, D. Simonian, M. P. Sarachik, W. Mason, and J. E. Furneaux, Phys. Rev. Lett. **77**, 4938 (1996).
[17] V. M. Pudalov, G. Brunthaler, A. Prinz, and G. Bauer, Pis'ma Zh. Eksp. Teor. Fiz. **68**, 415 (1998) [JETP Lett. **68**, 442 (1998)].
[18] K. M. Cham and R. G. Wheeler, Phys. Rev. Lett. **44**, 1472 (1980).
[19] R. Smith and P. Stiles, Solid State Commun. **58**, 511 (1986).
[20] S. Das Sarma and E. H. Hwang, Phys. Rev. B **61**, R7838 (2000); H. Min, E. H. Hwang, and S. Das Sarma, *ibid.* **86**, 085307 (2012).
[21] S. Das Sarma and E. H. Hwang, Phys. Rev. B **68**, 195315 (2003).
[22] V. Pudalov, G. Brunthaler, A. Prinz, and G. Bauer, Pis'ma Zh. Eksp. Teor. Fiz. **68**, 497 (1998) [JETP Lett. **68**, 534 (1998)].
[23] V. M. Pudalov, G. Brunthaler, A. Prinz, and G. Bauer, Phys. Rev. B **60**, R2154 (1999).
[24] S. Das Sarma and E. H. Hwang, Phys. Rev. Lett. **83**, 164 (1999).
[25] S. Das Sarma and E. H. Hwang, Phys. Rev. B **69**, 195305 (2004).
[26] B. L. Altshuler, G. W. Martin, D. L. Maslov, V. M. Pudalov, A. Prinz, G. Brunthaler, and G. Bauer, arXiv:cond-mat/0008005.
[27] B. Altshuler, D. Maslov, and V. Pudalov, Phys. E (Amsterdam) **9**, 209 (2001).
[28] O. Prus, M. Reznikov, U. Sivan, and V. Pudalov, Phys. Rev. Lett. **88**, 016801 (2001).
[29] L. A. Tracy, E. H. Hwang, K. Eng, G. A. Ten Eyck, E. P. Nordberg, K. Childs, M. S. Carroll, M. P. Lilly, and S. Das Sarma, Phys. Rev. B **79**, 235307 (2009).
[30] G. M. Minkov, A. V. Germanenko, and I. V. Gornyi, Phys. Rev. B **70**, 245423 (2004).
[31] A. Y. Kuntsevich, N. N. Klimov, S. A. Tarasenko, N. S. Averkiev, V. M. Pudalov, H. Kojima, and M. E. Gershenson, Phys. Rev. B **75**, 195330 (2007).
[32] G. Brunthaler, A. Prinz, G. Bauer, and V. M. Pudalov, Phys. Rev. Lett. **87**, 096802 (2001).
[33] M. Y. Simmons, A. R. Hamilton, M. Pepper, E. H. Linfield, P. D. Rose, D. A. Ritchie, A. K. Savchenko, and T. G. Griffiths, Phys. Rev. Lett. **80**, 1292 (1998).
[34] P. T. Coleridge, A. S. Sachrajda, and P. Zawadzki, Phys. Rev. B **65**, 125328 (2002).
[35] M. Rahimi, S. Anissimova, M. R. Sakr, S. V. Kravchenko, and T. M. Klapwijk, Phys. Rev. Lett. **91**, 116402 (2003).
[36] B. N. Narozhny, G. Zala, and I. L. Aleiner, Phys. Rev. B **65**, 180202(R) (2002).
[37] R. A. Davies and M. Pepper, J. Phys. C: Solid State Phys. **16**, L353 (1983).
[38] S. Kawaji, Surf. Sci. **170**, 682 (1986).
[39] A. V. Germanenko, G. M. Minkov, and O. E. Rut, Phys. Rev. B **64**, 165404 (2001).
[40] B. Altshuler, D. Maslov, and V. Pudalov, Phys. Status Solidi B **218**, 193 (2000).
[41] A. Lewalle, M. Pepper, C. J. B. Ford, E. H. Hwang, S. Das Sarma, D. J. Paul, and G. Redmond, Phys. Rev. B **66**, 075324 (2002).
[42] A. Lewalle, M. Pepper, C. J. B. Ford, D. J. Paul, and G. Redmond, Phys. Rev. B **69**, 075316 (2004).
[43] S. Das Sarma and E. H. Hwang, Phys. Rev. B **88**, 035439 (2013).
[44] S. D. Sarma and E. H. Hwang, Phys. Rev. B **89**, 235423 (2014).